



# The reliable sampling interval for monitoring interannual variability of the Kuroshio transport at 18°N

Jing Huang<sup>a,b</sup>, Linlin Zhang<sup>b,c,d,\*</sup>, Shanliang Zhu<sup>a</sup>, Jie Wu<sup>b,d</sup>, Xiaomei Yan<sup>b,c,d</sup>, Weiqi Song<sup>b,d</sup>, Shuguo Yang<sup>a</sup>

<sup>a</sup> School of Mathematics and Physics, Research Institute for Mathematics and Interdisciplinary Sciences, Qingdao University of Science and Technology, Qingdao 266100, China

<sup>b</sup> Key Laboratory of Ocean Circulation and Waves, Institute of Oceanology, Chinese Academy of Sciences, Qingdao 266071, China

<sup>c</sup> Lao Shan Laboratory, Qingdao 266237, China

<sup>d</sup> University of Chinese Academy of Sciences, Beijing 100049, China

## ARTICLE INFO

### Keywords:

Kuroshio

Interannual variability

Sampling interval

Intraseasonal variability

## ABSTRACT

The sampling interval for reliably monitoring interannual variability of the Kuroshio transport was studied using satellite altimeter data and outputs from HYbrid Coordinate Ocean Model (HYCOM). Interannual variations of the Kuroshio velocity and transport crossing 18°N were derived with different sampling interval, and their deviations from the ‘true’ interannual signals derived from original time series were estimated. The results indicate that sampling with an interval shorter than 20 days is required to obtain the reliable interannual signals, i.e., the Root Mean Square of the deviation is <50% of the interannual signal. However, the longer sampling intervals will lead to serious aliasing and degradation of the true interannual signals, which is mainly attributed to the energetic intraseasonal oscillations in this region. Power spectrum analysis reveal that there are significant 80-day intraseasonal variations as well as semiannual fluctuations in the Kuroshio transport at 18°N, which brings substantial sampling deviations relative to the true interannual variation. An ideal experiment is constructed to confirm that the reliable sampling interval of around 20 days, which can capture interannual variations and resolve the intraseasonal oscillation of the Kuroshio reliably at 18°N. This study provides an important reference for the future monitoring of the interannual variation of the Kuroshio.

## 1. Introduction

The Kuroshio is an important western boundary current of the subtropical ocean circulation system in the North Pacific. It originates east of the Philippines and is formed by the northern branch of the North Equatorial Current (NEC) in the western tropical Pacific Ocean (e.g., Nitani, 1972; Qu and Lukas, 2003; Fig. 1a). Kuroshio carries abundant high temperature and high salinity water northward, playing an important role in the large-scale ocean circulation and climate variability (Lukas et al., 1996; Hu et al., 2020).

Many studies have focused on the velocity and transport of Kuroshio with mooring and hydrographic observations in the Kuroshio origin area. Based on acoustic Doppler current profiler (ADCP) data at about 18°N, the maximum mean velocity exceeds 1.0 m/s in the upper 100 m (Lien et al., 2015). For the annual mean transport in the origin area, various estimates have been made: 15 Sv (1 Sv = 10<sup>6</sup> m<sup>3</sup>/s) by Lien et al.

(2014) with ADCP data during June 2012 to June 2013, 14 Sv by Qu et al. (1998) based on hydrographic (conductivity-temperature-depth, CTD) measurements from 1986 through 1990, 23.7 Sv by Ichikawa and Beardsley (1993) using the hydrographic and surface current data during 1986–1988, 27.6 Sv from Yaremchuk and Qu (2004) by combining hydrographic data, satellite altimetry and other data. Because of different sampling frequency and observation period, the Kuroshio transport east of the Luzon has significant differences.

Kuroshio is subject to multi-timescale variability, ranging from intraseasonal to interannual time scales. Based on mooring measurements at 18°N, Hu et al. (2013) and Ma et al. (2022) found that the Kuroshio and Luzon Undercurrent (LUC) beneath have significant intraseasonal variability with a period of 70–80 days. On seasonal timescale, the analysis based on observations and numerical simulations showed that Kuroshio at 18°N has a stronger (weaker) transport in spring (fall) (Yaremchuk and Qu, 2004; Qiu and Lukas, 1996; Qu et al.,

\* Corresponding author at: Key Laboratory of Ocean Circulation and Waves, Institute of Oceanology, Chinese Academy of Sciences, Qingdao 266071, China.  
E-mail address: [zhanglinlin@qdio.ac.cn](mailto:zhanglinlin@qdio.ac.cn) (L. Zhang).

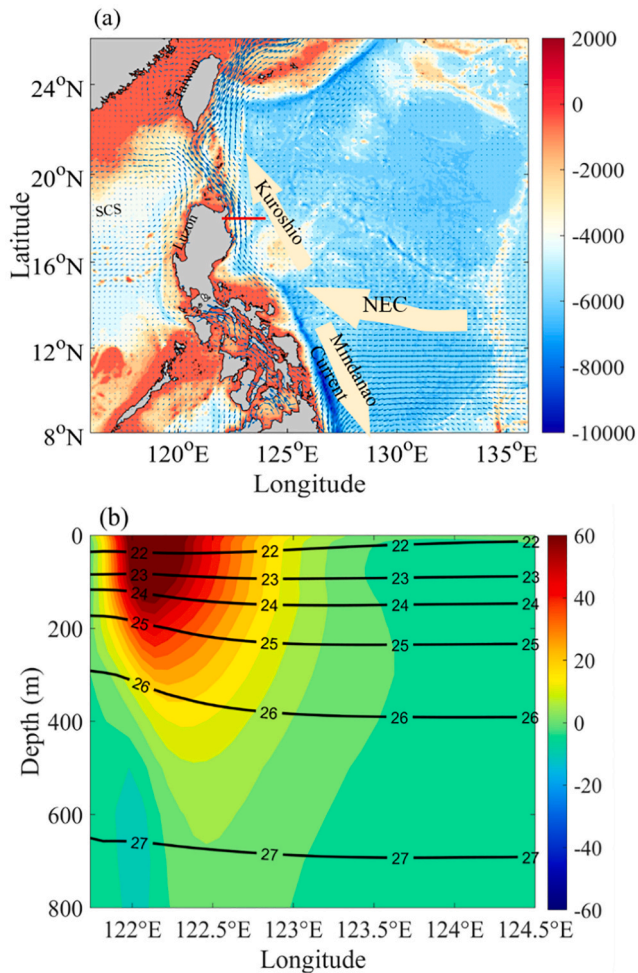


**Fig. 1.** (a) The bathymetry (colour, unit: m) of the study area. Vectors denote the mean surface velocity from satellite altimetry. Red line indicates the 18°N section. (b) The mean meridional velocity (colour, unit: cm/s) with potential density (contours, units:  $\text{kg}/\text{m}^3$ ) crossing the 18°N section from HYCOM outputs. Positive indicates northward velocity. (For interpretation of the references to colour in this figure legend, the reader is referred to the web version of this article).

1998; Wang et al., 2022a, 2022b). Used ADCP data at the Luzon Strait during June 2012 to June 2013, Lien et al. (2014) suggested that Kuroshio across the 18.75°N section has obvious seasonal variation with positive anomaly (i.e., an enhanced Kuroshio transport) in winter and spring, and negative in summer and autumn. In general, although most studies show that the Kuroshio transport increases in spring, some studies indicate that the Kuroshio transport increases in winter.

With regard to the interannual variability of the Kuroshio, previous studies suggested that the interannual variability of Kuroshio east of the Luzon Island is highly correlated with El Niño-Southern Oscillation (ENSO). During El Niño (La Niña) events, the NEC bifurcation shifts northward(southward) due to cyclonic/anticyclonic in the gyre, which leads to the decreased(increased) Kuroshio transport. (e.g., Qiu and Lukas, 1996; Kim et al., 2004; Zhai and Hu, 2012; Zuo et al., 2012; Chen et al., 2015; Hu et al., 2020). Nevertheless, several studies suggested that the interannual variation of Kuroshio does not correspond perfectly with ENSO. Qiu and Lukas (1996) mentioned that not all the interannual peaks of the Kuroshio transport correspond to the ENSO events. Based on satellite altimeter and sea level data of Keelung and Ishigaki from 1980 to 2008, Chang and Oey (2012) pointed out that the Kuroshio transport off Taiwan northeastern coast is dominated by Philippines-Taiwan Oscillation (PTO), and ENSO could only explain its partial interannual

variation.

In general, the above studies indicate that there exists some debate about the interannual variation of Kuroshio, which may be related to different locations, time periods, observation tools and sampling interval in the observation. In particular, hydrographic observations with coarse sampling interval might obtain inconsistent interannual variations. For example, using 14 times uneven seasonal or annual survey sampling at 18°N from 1986 to 1990, Qu et al. (1998) indicated that the minimum transport of Kuroshio occurred during the mature phase of the 1986–1987 El Niño, which is nearly out of phase with Lukas (1988) and Qiu and Joyce (1992). In addition, Yaremchuk and Qu (2004) proposed that transport estimates derived from observational evidence east of Luzon Island were uncertain due to the lack of long-term velocity measurements. In fact, in addition to different locations, time periods and observation tools, the coarse sampling interval in the observation (especially the hydrographic observation) might affect the estimate of the interannual variation of the Kuroshio. Particularly, there are strong seasonal, intraseasonal or even higher frequency fluctuations in the Kuroshio as mentioned above. But the common sampling interval of hydrographic observation is seasonally or even annually, which significantly misses those high-frequency signals and leads to misinterpretations of the Kuroshio interannual variation.

The purpose of this study is to quantify the aliasing errors or RMSE at different sampling intervals and find a reasonable or reliable sampling interval for monitoring the interannual variation of the Kuroshio transport. Gilson and Roemmich (2002) have suggested that raising the sampling frequency to monthly or even fortnightly could improve the observing system for western boundary currents. Theoretically, a higher sampling frequency of observation would monitor the interannual variation preferably, while inadequate sampling of oceanic motions, which commonly occurs for oceanic measurements, could cause peculiar spectral feature and potentially lead to obvious misinterpretations (Wang et al., 2022a, 2022b). Although satellite altimetry is characterized by its high temporal and spatial resolution, only surface information of the Kuroshio could be provided. Previous cruise surveys on the Kuroshio were usually conducted once a year, and such coarse sampling might induce significant alias in the estimation of the Kuroshio interannual variations. Exploring a reasonable sampling interval for reliably monitoring the interannual variation of Kuroshio transport is of significant importance for both observing and investigating the multi-scale variation of the Kuroshio. The results of this study provide basis for understanding the uncertainty in the Kuroshio interannual variability estimated with sparse observations, and it also provides reference for the future design of hydrographic observations like CTD or Glider transects.

Here we analyzed the sampling interval required to reliably monitor the interannual variation in the Kuroshio. The satellite altimetry and HYCOM outputs as well as the methods were described in section 2. The original time series of surface velocity and cross-section transport derived from the data were presented in section 3.1. Section 3.2 mainly introduced the sampling interval needed to minimize the interannual deviation between the subsampling time series and the original time series. An ideal experiment was conducted in section 3.3 to verify the reliable sampling interval. A summary was given in section 4.

## 2. Data and method

### 2.1. Satellite altimetry

Sea surface geostrophic velocities derived from the satellite altimeter-measured sea surface height was used to obtain the interannual variability of the Kuroshio velocity. The daily surface geostrophic velocity data at  $0.25^\circ \times 0.25^\circ$  resolution during 1998 to 2021 was obtained from Archiving Validation and Interpretation of Satellite Data in Oceanography (AVISO) from the website at <http://www.aviso.oceanobs.com/>. Technical details on AVISO product data processing can be found in Rio et al. (2011) and Ducet et al. (2000).

## 2.2. HYCOM outputs

The global ocean circulation model outputs from HYCOM (HYbrid Coordinate Ocean Model) was also used in this study. The model is HYCOM GLBv0.08 and uses mixed coordinates (isopycnic coordinates,  $\sigma$  coordinates, and  $z$  coordinates) in the vertical, allowing appropriate coordinates in different layers of the ocean. HYCOM assimilates horizontal flow field, sea surface and thermohaline information from multiple observational sources. The horizontal resolution of the model is  $0.08^\circ \times 0.08^\circ$ , and there are 36 layers from 5 m to 2000 m in the vertical direction. The outputs in the upper 800 m within  $110^\circ\text{E}$ - $130^\circ\text{E}$ ,  $15^\circ\text{N}$ - $30^\circ\text{N}$  during 1998–2021 were used in the following analysis. Details of the HYCOM outputs can be found in [Chassignet et al. \(2007\)](#). It is worth nothing that the main reason for using HYCOM outputs is that it has three-dimensional current velocities, long-time scale and high resolution, which enables us to investigate the impact of sampling interval on the estimation of interannual variability of the Kuroshio. Moreover, HYCOM outputs have been extensively used in previous studies to explore the structure and variability of the Kuroshio in this region (e.g., [Wang et al., 2009](#); [Wu et al., 2020](#)).

## 2.3. Estimation of reliable sampling interval

The Kuroshio originates from the northern branch of the NEC off the eastern coast of the Luzon Island, and the  $18^\circ\text{N}$  section is often chosen to investigate the Kuroshio ([Fig. 1a](#)). In this study, we focused on this section to estimate the reliable sampling interval for monitoring the interannual variability of the current. At  $18^\circ\text{N}$ , the Kuroshio spans from  $122^\circ$  to  $124^\circ\text{E}$  and extends from the surface down to 800 m, with its maximum velocity reaching up to 70 cm/s at the depth around 100 m ([Fig. 1b](#)). A similar method has been used in [Meredith and Hughes \(2005\)](#) to investigate the sampling interval for monitoring interannual variability of the Antarctic Circumpolar Current transport. The annual mean time series of the surface meridional velocity crossing the  $18^\circ\text{N}$  section between  $122^\circ$ - $124^\circ\text{E}$  was derived with the daily data from satellite altimetry and HYCOM, respectively, which is regarded as the true interannual signal of the Kuroshio velocity. Similarly, we estimated the true interannual signal of the Kuroshio transport by averaging the daily transport year by year, while the daily transport was calculated with the integration of all the meridional velocities. The formula for the meridional transport of Kuroshio in the upper 800 m between  $122^\circ$ - $124^\circ\text{E}$  is

$$VT = \int_{122^\circ\text{E}}^{124^\circ\text{E}} \int_{800\text{m}}^0 V dz dx,$$

and the formula for the Kuroshio transport within isopycnals between 22

$$\text{and } 26.8 \text{ kg/m}^3 \text{ is } VT = \int_{122^\circ\text{N}}^{124^\circ\text{N}} \int_{22\text{kg/m}^3}^{26.8\text{kg/m}^3} V dz dx.,$$

Here,  $V$  is the meridional velocity.

In order to obtain the reliable sampling interval for monitoring the Kuroshio interannual variation, firstly we subsampled the original daily time series with different intervals ranging from 1 to 180 days. Note that for each sampling interval, there are different initial days of sampling (e.g., for the 5-day sampling interval, there are five possible initial days to generate five different subsampled time series). Then, the Root Mean Square Error (RMSE) between the interannual signal derived from the subsampled time series and the true interannual signal was calculated, representing the deviation of the subsampled time series relative to the true interannual signal. In practical measurements, the sampling frequency of observations is always finite. The true series could only be substituted by the most reliable (best) series. RMSE is sensitive to larger or smaller errors in a group of measurements, which can reflect the precision of the measurement. The RMSE are primarily controlled by the following equations:

$$RMSE = \sqrt{\frac{\sum_{i=1}^n (x_{obs,i} - x_{model,i})^2}{n}}$$

Here,  $n$  is the number of years, and  $x$  represents the velocity and transport. For each sampling interval, the corresponding RMSE is the average of that generated by all possible initial days of sampling. When the RMSE is  $<50\%$  of the standard deviation (STD) of the true interannual signal, we suggest that the corresponding subsampling is able to capture the interannual signal reliably. The STD can be written as

$$STD = \sqrt{\frac{\sum_{i=1}^n (x_i - \bar{x})^2}{n}}$$

The ratio of RMSE and STD can reveal the magnitude of errors between the subsampled time series and the true time series.

## 3. Results

### 3.1. 'True' interannual variation of Kuroshio velocity and transport

[Fig. 2a](#) shows the Kuroshio velocity time series of satellite altimetry and HYCOM outputs at  $18^\circ\text{N}$  section during 1998–2021, respectively. The Kuroshio transport is calculated from HYCOM outputs as the integration of all the meridional velocities in the upper 800 m and with within isopycnals between 22 and  $26.8 \text{ kg/m}^3$  between  $122^\circ$ - $124^\circ\text{E}$  at  $18^\circ\text{N}$ . After averaging per year, the obtained annual time series is shown in [Fig. 2b](#) and [d](#). The mean surface velocity of Kuroshio derived from satellite altimetry is 37.0 cm/s, and that from HYCOM outputs is 42.5 cm/s. These results are basically consistent with [Zuo et al. \(2012\)](#) who calculated the annual mean velocity of the Kuroshio at  $18^\circ\text{N}$  year by year during 1993–2008, and the annual mean time series ranges from 33 cm/s to 39 cm/s (see their [Fig. 12](#)). As for the Kuroshio transport, regardless of a systematic difference around 1 Sv, the transports derived from the two methods exhibit consistent interannual variations ([Fig. 2c](#)-[2d](#)), and their correlation reaches 0.92. The mean transport derived in the upper 800 m is about 24.69 Sv and within isopycnals between 22 and  $26.8 \text{ kg/m}^3$  is 23.54 Sv, very close to the transport of 23.7 Sv by [Ichikawa and Beardsley \(1993\)](#) using the hydrographic and surface current data during 1986–1988, 21.4 Sv derived from hydrographic surveys from September 1987 and April by [Toole et al. \(1990\)](#). The annual mean time series of velocity in [Fig. 2b](#) and transport in [2d](#) by calculating the velocity in the upper 800 m are regarded as the true interannual signals of Kuroshio.

Significant interannual variations of the Kuroshio could be observed in the annual mean time series. There is significant decadal variability accompanied with moderate interannual signals in the annual mean time series of surface velocity shown in [Fig. 2b](#), while the time series of Kuroshio transport in [Fig. 2d](#) seem to be dominated by interannual variations. Nevertheless, this study does not intend to distinguish the interannual and decadal variations strictly in this study, and mainly focuses on the year-to-year variation of the Kuroshio. The STD of the annual mean time series of surface velocity from satellite altimetry and HYCOM are 2.63 cm/s and 3.65 cm/s, respectively. The STD of transport between 0 and 800 m from HYCOM reaches 4.04 Sv. In addition, it is worth pointing out that the original daily time series of both velocity and transport exhibits energetic high-frequency fluctuations, which appears even stronger compared with the interannual signals ([Fig. 2a](#) and [c](#)). Under the coarse sampling, these high frequency fluctuations could generate significant deviations in the subsampled series and results in large errors in resolving the interannual variations. Therefore, to obtain the reliable interannual variations, the sampling interval should be as short as possible to resolve those high frequency fluctuations.

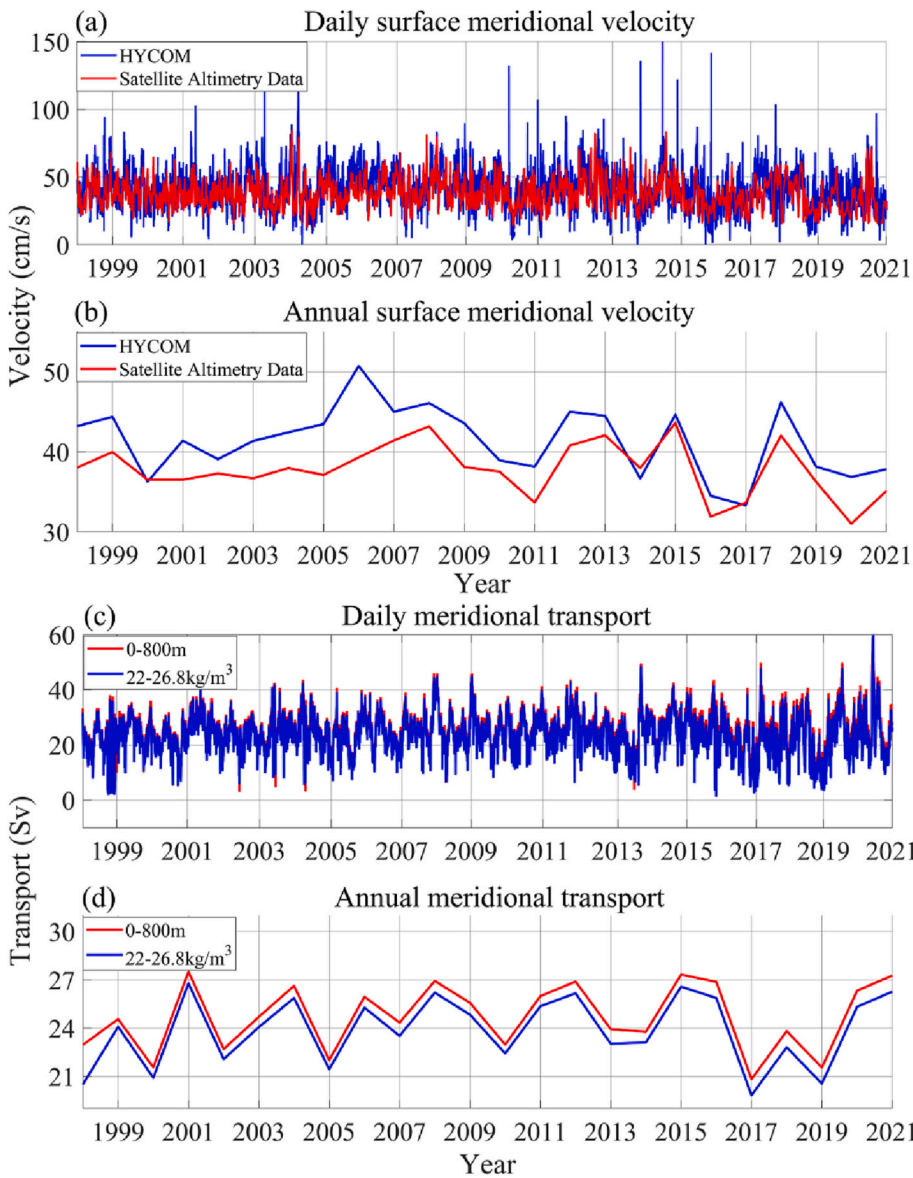


**Fig. 2.** (a) The daily time series of surface meridional velocity averaged between 122°E and 124°E along the 18°N section derived from satellite altimetry data (red) and HYCOM outputs(blue). (b) is the same as (a), but for the annual mean time series. (c) The daily time series of meridional transport in the upper 800 m (red) and in the isopycnal range of 22–26.8 kg/m<sup>3</sup> (blue) between 122°–124°E along the 18°N section. (d) is the same as (c), but for the annual mean time series. (For interpretation of the references to colour in this figure legend, the reader is referred to the web version of this article).

### 3.2. Reliable sampling interval for monitoring interannual variability

To investigate the reliable sampling interval for monitoring the interannual variability in Kuroshio, the RMSE between the new annual time series and true interannual series was calculated according to the method at section 2.3 and plotted as a function of sampling interval (Fig. 3a, b,3c). Obviously, the larger the sampling interval is, the larger the RMSE is. According to the criterion of RMSE <50% of the interannual STD, to capture the interannual variations of Kuroshio surface velocity derived from satellite altimetry, the required sampling interval is ~22 days. Under the criterion of RMSE equaling to the interannual STD, the sampling interval is ~40 days. In the case of HYCOM outputs, the corresponding reliable sampling interval is ~20 days (RMSE = 0.5 × STD) and 38 days (RMSE = 1 × STD) in terms of surface velocity and ~22 days (RMSE = 0.5 × STD), ~48 days (RMSE = 1 × STD) in terms of transport.

According to Fig. 3, this study derived two functions representing the relationship between RMSE and sampling interval for surface velocity and transport using second-order polynomial fitting method, which are shown as follows:

$$\text{velocity} : Rv(x) = 1.23SI^2 + 1.47SI + 3.04$$

$$\text{transport} : Rt(x) = 0.93SI^2 + 2.92SI + 1.49$$

Here, R is the ratio of RMSE and STD and SI is sampling interval.

Nevertheless, the functions are derived from velocity and transport at 18°N, and its applicability at other latitudes or in other regions still needs further investigation, because the variation of currents is strongly region-dependent.

To demonstrate the reliability of the above sampling interval in capturing the true interannual signals, the newly subsampled time series for all possible initial days when RMSE = 0.5 × STD (Fig. 4a, c, e) and RMSE = 1 × STD were compared with the true interannual time series (Fig. 4b, d, f). One can see that both subsampled series with RMSE = 0.5 × STD and that with RMSE = 1 × STD are generally consistent with the true interannual time series, with the former being closer to the true series. Another can see that the subsampled series with RMSE = 0.5 × STD are generally tight with the true series, and that with RMSE = 1 × STD are scattered with the true interannual time series. This phenomenon also indicates the deviation between the subsampled series and the true series when RMSE = 0.5 × STD is letter than when RMSE = 1 ×

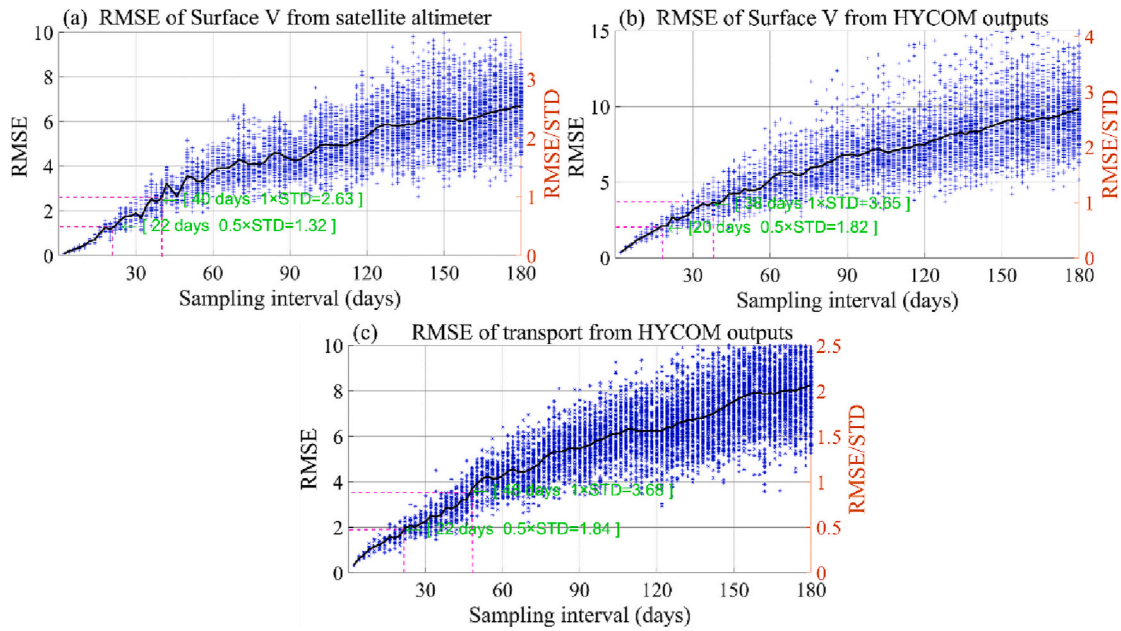


**Fig. 3.** The RMSE between subsampled time series and true time series of surface velocity derived from satellite altimetry (a) and HYCOM data (b) at different sampling intervals. (c) is the same as (a), but for transport. Blue dots represent the RMSE at different sampling intervals and different initial days. Averaging the RMSE generated by all possible initial days at each sampling interval obtains the black line. The sampling intervals when  $RMSE = 0.5 \times STD$ ,  $1 \times STD$ , are marked in green respectively. STD represents the standard deviation of the true annual time series. (For interpretation of the references to colour in this figure legend, the reader is referred to the web version of this article).

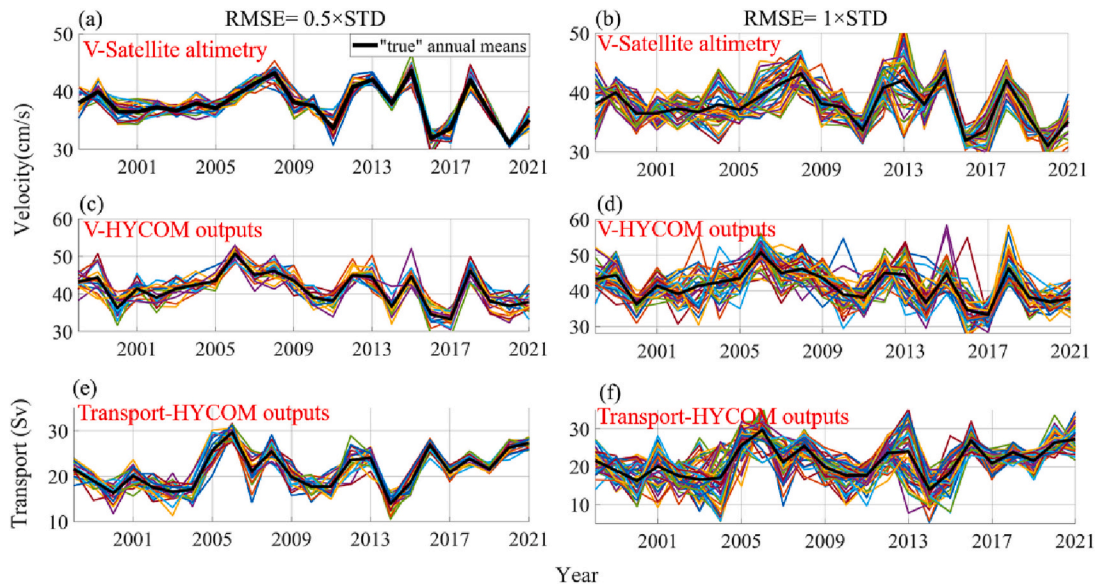


**Fig. 4.** The annual mean subsampled time series under all possible initial days when the sampling interval is around 20 days ( $RMSE = 0.5 \times STD$ , left panels) and 40 days ( $RMSE = 1 \times STD$ , right panels). The true annual mean time series is shown as the bold black curve.

**Table 1**  
The sampling interval for monitoring the interannual variability of the Kuroshio.

	Surface V from satellite altimeter		Surface V of HYCOM		HYCOM transport	
	RMSE (cm/s)	sampling interval (days)	RMSE (cm/s)	sampling interval (days)	RMSE (Sv)	sampling interval (days)
$0.5 \times STD$	1.32	22	1.83	20	1.84	22
$1 \times STD$	2.63	40	3.65	38	3.68	48

STD. These results indicate that the sampling interval around ~20 days, with  $RMSE = 0.5 \times STD$ , is able to capture the interannual variations of the Kuroshio velocity and transport to a reliable extent.

Table 1 summarized the sampling interval when the corresponding RMSE is equal to 50% and 100% of the STD of the true interannual signal derived from satellite altimetry and HYCOM, respectively. The results for surface velocity and transport from satellite data and HYCOM generally agree well with each other. All of them indicate that the required sampling interval is about 20 days and 40 days when the RMSE is equal to  $0.5 \times STD$  and  $1 \times STD$ , respectively. Therefore, we suggest that the reliable sampling interval for monitoring the interannual variation of Kuroshio velocity and transport is about 20 days even shorter than 20 days. Nevertheless, it is inescapable that the 20-day repeated sampling also has deviations in reality, but that deviation is only around 50% of the true interannual signal.

To further verify the reliable sampling interval mentioned above, the correlation coefficient between the subsampled time series and the true interannual series was calculated and shown as a function of sampling interval (Fig. 5). Here, the subsampled time series generated with all the possible initial days were considered, and Fig. 5 presents the mean correlation coefficient corresponding to each sampling interval. Obviously, the correlation decreases significantly with the increase of sampling interval, indicating that the coarser sampling interval induces larger bias or deviations from the true interannual signal. When the sampling interval is ~20 days ( $RMSE = 0.5 \times STD$ ), the average correlation coefficient for both velocity and transport is above 0.86, confirming that the subsampled time series well captures interannual variability of the Kuroshio. When the sampling interval is around 40 days, the corresponding correlation coefficient is around 0.7, which is above the 95% significance level statistically (is around 0.5, shown with red line in Fig. 5). But the corresponding RMSE or aliasing error of the subsampled time series is equal to 100% of the STD (Fig. 3). The annual mean subsampled time series also exhibit large deviations from the 'true' interannual signals (Fig. 4b, d and f). Considering both the correlation coefficient and aliasing error, this study suggest that the sampling interval of 40 days (correlation coefficient of 0.7,  $RMSE = 1 \times STD$ ) is not acceptable. Generally speaking, a sampling interval <20 days is required in order to monitor the interannual variation of the Kuroshio accurately.

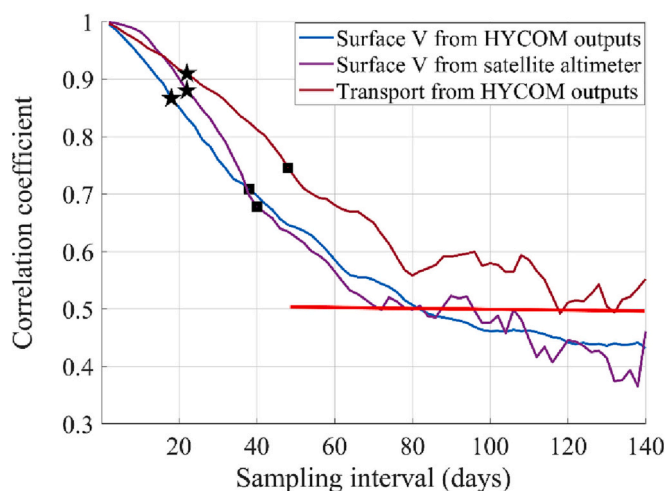


Fig. 5. The correlation between the annual mean subsampled time series and the annual mean true time series at different sampling intervals. The correlation is a mean value considering all the possible subsampled time series under different initial days. ★, ■ and red line denote the correlation coefficient corresponding to  $RMSE = 0.5 \times STD$ ,  $RMSE = 1 \times STD$  and the 95% significance level, respectively. (For interpretation of the references to colour in this figure legend, the reader is referred to the web version of this article).

### 3.3. Ideal experiment

Why is the reliable sampling interval around 20 days for monitoring interannual variability of the Kuroshio at 18°N? We attempt to explore the physical process behind it. The power spectral density of velocity from HYCOM indicates energetic fluctuations on intraseasonal (50–100 days), semiannual (~180 days), annual (~360 days), and interannual (~3 years) time scales (Fig. 6b), while that from satellite altimetry also exhibits significant peaks on intraseasonal and annual time scales (Fig. 6a). Moreover, the satellite altimetry results show obvious peaks on semiannual and interannual time scales, but they are below the 95% significance level. The possible reason for the insignificance of the semiannual and interannual signals is as follows: Due to the energetic multiple-scale processes (particularly intraseasonal oscillations) in the real ocean and relatively smoother results simulated by numerical models, satellite altimetry results exhibit relatively higher power spectrum density compared with the HYCOM results (Fig. 6a-6b). Statistically, higher power spectrum density corresponds to higher background spectrum of red noise or higher significance level, as shown by the significance level in Fig. 6a. The semiannual and interannual signals captured by satellite altimetry seems not strong enough to pass the significance test. These multi-scale fluctuations as shown by Fig. 6, could significantly affect the interannual signal of Kuroshio under different sampling intervals. Particularly, the high frequency fluctuations with period around 50–100 days is hypothesized as a key factor to determine the reliable sampling interval of 20 days, because this interval is probably needed to resolve the intraseasonal fluctuations and reduce the sampling deviations.

To testify this hypothesis, an ideal daily time series was firstly synthesized by superimposition of three sinusoidal time series with periods of ~80 days, ~180 days and ~360 days, respectively. The formula for constructing time series can be expressed as

$$TS = m \sin\left(\frac{2\pi}{T} t\right)$$

Here,  $TS$  represents time series,  $m$  represents the amplitude,  $T$  represents the period,  $t$  represents time.

The amplitude of each sinusoidal sequence was set to be consistent with that of the corresponding band-pass filtered surface velocity from satellite altimetry. Then, the original velocity time series from satellite altimetry after 2–7 years' band-pass filtering was superimposed onto the ideal time series, and the obtained one was considered as the ideal original time series named A (Fig. 7a). Following similar procedures to that in section 3.2, the RMSE of the subsampled time series from A were estimated and plotted as a function of sampling interval (Fig. 7c). According to the criterion ( $RMSE = 0.5 \times STD$ ) mentioned in the section 3.2, the reliable sampling interval for obtaining the interannual signal of time series A is ~28 days, indicating that it requires around 28 days to resolve the intraseasonal fluctuations and capture the interannual variability reliably (See Table 2). The higher frequency oscillations with period shorter than 80 days may need relatively shorter sampling interval (around 20 days) to be resolved. In contrast, the ideal time series is more regular, and the dominant period of the intraseasonal signal is around 80 days, which is less contaminated by higher frequency oscillations. Therefore, a relatively longer sampling interval like 28 days can resolve this signal properly. This result generally agrees with the reliable sampling interval of ~20 days estimated with the satellite altimetry and HYCOM outputs in section 3.2.

In addition to the effect of high frequency oscillations, could the intensity change of interannual signal influence the reliable sampling interval? To investigate this issue, the amplitude of interannual component in time series A was doubled and the new series was named B (Fig. 7b). For time series B, the required sampling interval for reliably monitoring the interannual variation increases to 42 days. The remarkable increase of reliable sampling interval or reduction of

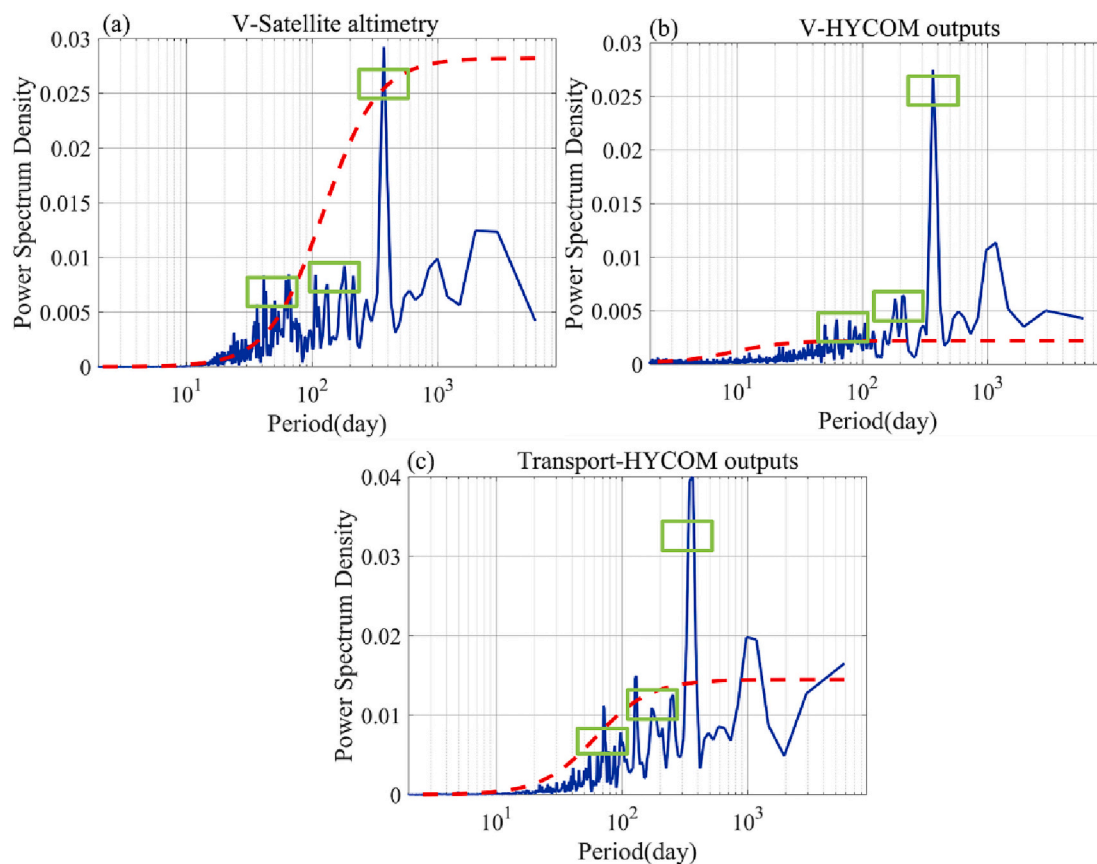


**Fig. 6.** Power spectral density (blue) of the mean meridional velocity time series between 122°–124°E at 18°N derived from (a) satellite altimetry, (b) HYCOM outputs. (c) is the same as (a) and (b), but for the meridional transport in the upper 800 m derived from HYCOM outputs. Red dashed curve indicates the 95% significance level. (For interpretation of the references to colour in this figure legend, the reader is referred to the web version of this article).

sampling interval can be explained by the fact that the intensification of interannual signal would weaken the effect of high-frequency fluctuations. Therefore, a relatively coarser sampling interval is able to capture the reliable interannual signals.

In addition, a prominent feature worth noting is that two peaks of RMSE appear at sampling interval of  $\sim 80$  days and  $\sim 160$  days (Fig. 7c and d). Generally speaking, these two peaks are related to the intraseasonal (period:  $\sim 80$  days) and semiannual (period:  $\sim 180$  days) signals contained in the ideal daily time series. As the sampling interval increases, the RMSE or aliasing error of the subsampled time series relative to the ideal daily time series becomes larger. When the sampling interval is increased to 60 or 140 days, the coarse sampling is unable to capture the intraseasonal or semiannual signals, which results in a sharp increase of RMSE. As for the decrease of RMSE between periods of 80–100 days and 160–200 days, we have no clear interpretation at this stage. It might be due to the fact that the intraseasonal and semiannual signals in the ideal time series are too regular, which will be investigated in further studies.

#### 4. Summary and discussion

The interannual variability of Kuroshio is of great importance in large-scale ocean circulation and climate change and has aroused extensive research interests. Monitoring interannual variability of Kuroshio reliably and reasonably is very important for the Kuroshio studies. Theoretically, the daily or even hourly sampling could accurately resolve the Kuroshio interannual variability, but is expensive and impractical. Therefore, determining a reliable and cost-effective sampling interval is necessary. Focusing on the 18°N section where the Kuroshio originates, the reliable sampling interval for monitoring the

Kuroshio interannual variability was investigated using satellite altimeter data and outputs from HYCOM. Under different sampling intervals, the deviations between the new subsampled time series of velocity and transport crossing the 18°N section and the true interannual time series were estimated. It is suggested that a sampling interval shorter than 20 days can capture the reliable interannual signals, with the Root Mean Square error of the subsampled time series being  $<50\%$  of the STD of the true interannual signal. The reliable sampling interval of  $\sim 20$  days was also confirmed by an ideal experiment. It was revealed that the sampling with an interval of shorter than 20 days can resolve the energetic intraseasonal fluctuations which significantly affect the interannual signal under the circumstance of coarse sampling.

In this study, we mainly focused on the 18°N section to explore the reliable sampling interval for monitoring the Kuroshio interannual variability. But whether the reliable sampling interval is region-dependent and the sampling intervals of monitoring different current variations also interests us. Actually, the reliable sampling interval depends on intense signals in the time series. Preliminary analyses indicate that the reliable sampling interval for monitoring the Kuroshio interannual variability exhibits salient geographic characteristics. Detailed physical processes beyond these different sampling intervals still remain unexplored, which will be addressed in future studies.

This study suggests that the required sampling interval to reliably monitor the interannual variability of Kuroshio is  $\sim 20$  days or shorter, which provides basis for understanding the uncertainty in the Kuroshio interannual variability estimated with sparse observations, and it also provides reference for the future design of hydrographic observations like CTD or Glider transects. Nevertheless, it also indicates that previous transect observations once or several times a year result in non-ignorable errors in resolving the interannual variations. Therefore, the

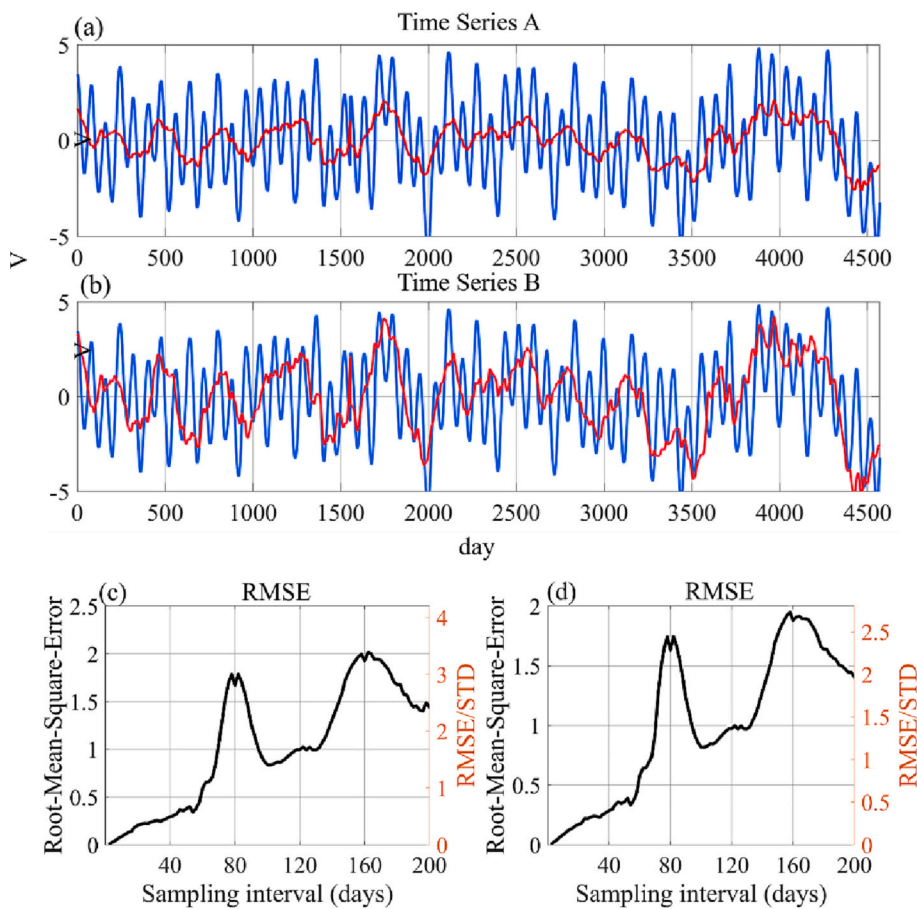


**Fig. 7.** (a) Ideal daily time series A synthesized by superimposition of three sinusoidal time series with periods of ~80 days, ~180 days and 2–7 years (red curve); (b) is the same as (a), but the interannual component (2–7 years) is doubled. (c) and (d) show the RMSE of the subsampled time series from time series A and B as a function of sampling interval (black curve), respectively. (For interpretation of the references to colour in this figure legend, the reader is referred to the web version of this article).

**Table 2**  
Sampling interval of time series A and B when RMSE is equal to  $0.5 \times \text{STD}$  and  $1 \times \text{STD}$ , respectively.

	A		B	
	RMSE (cm/s)	Sampling interval (days)	RMSE (cm/s)	Sampling interval (days)
$0.5 \times \text{STD}$	0.26	28	0.41	42
$1 \times \text{STD}$	0.52	56	0.83	68

integrated observations and analysis based are necessary for the reliable estimation of the interannual variation of the Kuroshio in the future.

**Declaration of Competing Interest**

The authors declare that the research was conducted in the absence of any commercial or financial relationships that could be construed as a potential conflict of interest.

**Data availability**

I have shared the link to my data at the section 2.

**Acknowledgments**

This study was supported by the National Key Research and Development Program of China (No. 2020YFA0608801), the National Natural Science Foundation of China (No. 41730534), the Strategic Priority Research Program of the Chinese Academy of Sciences (No. XDB42010105), and the National Natural Science Foundation of China

(No. 42122041). The TS Scholar Program (No. tsqn202103128), Laoshan Science and Technology Innovation project (No. LSKJ202201700) and NSFC Shiptime Sharing Projects (Nos. 42049909 and 42249909) also supported this study. This study was benefited from the freely available datasets: satellite altimetry dataset from the website on <http://www.avisio.oceanobs.com/>. The global ocean circulation model outputs from HYCOM (HYbrid Coordinate Ocean Model) GLBv0.08 was also used in this study.

**References**

Chang, Y.L., Oey, L.Y., 2012. The Philippines-Taiwan oscillation: monsoonlike interannual oscillation of the subtropical-tropical western North Pacific wind system and its impact on the ocean. *J. Clim.* 25 (5), 1597–1618. <https://doi.org/10.1175/JCLI-D-11-00158.1>.

Chassignet, E.P., Hulburt, H.E., Smedstad, O.M., Halliwell, G.R., Hogan, P.J., 2007. The HYCOM (HYbrid Coordinate Ocean Model) data assimilative system. *J. Mar. Syst.* 65 (1–4), 60–83. <https://doi.org/10.1016/j.jmarsys.2005.09.016>.

Chen, Z., Wu, L., Qiu, B., Li, L., Hu, D., Liu, C., Jia, F., Liang, X., 2015. Strengthening Kuroshio observed at its origin during November 2010 to October 2012. *J. Geophys. Res. Oceans* 120 (4), 2460–2470. <https://doi.org/10.1002/2014JC010590>.

Ducet, N., Traon, P., Reverdin, G., 2000. Global high-resolution mapping of ocean circulation from TOPEX/Poseidon and ERS-1 and -2. *J. Geophys. Res.* 105 (C8), 19477–19498. <https://doi.org/10.1002/2014JC010590>.

Gilson, J., Roemmich, D., 2002. Mean and temporal variability in Kuroshio geostrophic transport south of Taiwan (1993–2001). *J. Oceanogr.* 58, 183–195. <https://doi.org/10.1023/A:1015841120927>.

Hu, D., Hu, S., Wu, L., Li, L., Zhang, L., Diao, X., et al., 2013. Direct measurements of the Luzon undercurrent. *J. Phys. Oceanogr.* 43 (7), 1417–1425. <https://doi.org/10.1175/JPO-D-12-0165.1>.

Hu, D., Wang, F., Sprintall, J., Wu, L., Riser, S., Cravatte, S., et al., 2020. Review on observational studies of western tropical Pacific Ocean circulation and climate. *J. Oceanol. Limnol.* 38 (4), 906–929. <https://doi.org/10.1007/s00343-020-0240-1>.

Ichikawa, H., Beardsley, R.C., 1993. Temporal and spatial variability of volume transport of the Kuroshio in the East China Sea. *Deep Sea Res. Part I Oceanogr. Res. Papers.* 40 (3), 583–605. [https://doi.org/10.1016/0967-0637\(93\)90147-U](https://doi.org/10.1016/0967-0637(93)90147-U).

- Kim, Y.Y., Qu, T., Jensen, T., Miyama, T., Mitsudera, H., Kang, H.W., Ishida, A., 2004. Seasonal and interannual variations of the north equatorial current bifurcation in a high-resolution OGCM. *J. Geophys. Res. Oceans* 109 (C3), C03040. <https://doi.org/10.1029/2003JCO02013>.
- Lien, R.C., Ma, B., Cheng, Y.H., Ho, C.R., Qiu, B., Lee, C., Chang, M.H., 2014. Modulation of Kuroshio transport by mesoscale eddies at the Luzon Strait entrance. *J. Geophys. Res. Oceans* 119 (4), 2129–2142. <https://doi.org/10.1002/2013JC009548>.
- Lien, R.C., Ma, B., Lee, C.M., Sanford, T.B., Mensah, V., Centurioni, L.R., et al., 2015. The Kuroshio and Luzon undercurrent east of Luzon Island. *Oceanography* 28 (4), 54–63. <https://doi.org/10.5670/oceanog.2015.81>.
- Lukas, R., 1988. Interannual fluctuations of the Mindanao current inferred from sea level. *J. Geophys. Res.* 93 (C6), 6744–6748. <https://doi.org/10.1029/JC093iC06p06744>.
- Lukas, R., Yamagata, T., McCreary, J.P., 1996. Pacific low-latitude western boundary currents and the Indonesian throughflow. *J. Geophys. Res. Oceans* 101 (C5), 12209–12216. <https://doi.org/10.1029/96JC01204>.
- Ma, J., Hu, S., Hu, D., Villanoy, C., Wang, Q., Lu, X., Yuan, X., 2022. Structure and variability of the Kuroshio and Luzon undercurrent observed by a mooring array. *J. Geophys. Res. Oceans* 127 (2). <https://doi.org/10.1029/2021JC017754>.
- Meredith, M.P., Hughes, C.W., 2005. On the sampling timescale required to reliably monitor interannual variability in the Antarctic circumpolar transport. *Geophys. Res. Lett.* 32 (3), 431–449. <https://doi.org/10.1029/2004GL022086>.
- Nitani, H., 1972. Beginning of the Kuroshio. In: Stommel, H., Yoshida, K. (Eds.), *Kuroshio, its physical aspects*. University of Tokyo Press, Tokyo, Japan, pp. 129–163.
- Qiu, B., Joyce, T., 1992. Interannual variability in the mid- and low-latitude western North Pacific. *J. Phys. Oceanogr.* 22 (09), 1062–1079. [https://doi.org/10.1175/1520-0485\(1992\)022<1062:IVITMA>2.0.CO;2](https://doi.org/10.1175/1520-0485(1992)022<1062:IVITMA>2.0.CO;2).
- Qiu, B., Lukas, R., 1996. Seasonal and interannual variability of the north equatorial current, the Mindanao current, and the Kuroshio along the Pacific western boundary. *J. Geophys. Res. Oceans* 101 (C5), 12315–12330. <https://doi.org/10.1029/95JC03204>.
- Qu, T., Lukas, R., 2003. The bifurcation of the north equatorial current in the Pacific. *J. Phys. Oceanogr.* 33 (1), 5–18. [https://doi.org/10.1175/1520-0485\(2003\)033<0005:TB\\_OTNE>2.0.CO;2](https://doi.org/10.1175/1520-0485(2003)033<0005:TB_OTNE>2.0.CO;2).
- Qu, T., Mitsudera, H., Yamagata, T., 1998. On the western boundary currents in the Philippine Sea. *J. Geophys. Res.* 103 (C4), 7537–7548. <https://doi.org/10.1029/98JC00263>.
- Rio, M.H., Guinehut, S., Larnicol, G., 2011. New CNES-CLS09 global mean dynamic topography computed from the combination of GRACE data, altimetry, and in situ measurements. *J. Geophys. Res.* 116 (C7), C07018. <https://doi.org/10.1029/2010JC006505>.
- Toole, J.M., Millard, R.C., Wang, Z., Pu, S., 1990. Observations of the Pacific north equatorial current bifurcation at the Philippine coast. *J. Phys. Oceanogr.* 20 (2), 307–318. [https://doi.org/10.1175/1520-0485\(1990\)020<0307:OOTPNE>2.0.CO;2](https://doi.org/10.1175/1520-0485(1990)020<0307:OOTPNE>2.0.CO;2).
- Wang, Q., Cui, H., Zhang, S., Hu, D., 2009. Water transports through the four main straits around the South China Sea. *Chin. J. Oceanol. Limnol.* 27 (2), 229–236. <https://doi.org/10.1007/s00343-009-9142-y>.
- Wang, C., Liu, Z., Lin, H., 2022a. Interpreting consequences of inadequate sampling of oceanic motions. *Limnol. Oceanogr. Letters* 7 (5), 385–391. <https://doi.org/10.1002/lol2.10260>.
- Wang, F., Zhang, L., Feng, J., Hu, D., 2022b. Seasonal variability of the north equatorial current–Kuroshio current–Mindanao current based on observations. *Front. Mar. Sci.* 9, 2296–7745. <https://doi.org/10.3389/fmars.2022.1023020>.
- Wu, J., Zhang, L., Yan, X., 2020. Comparative analysis of seasonal and interannual variation of Kuroshio east of Luzon and Taiwan Island. *J. Oceanol. Limnol.* 51 (4), 839–850. <https://doi.org/10.11693/hyhz20200300062>. (In Chinese).
- Yaremchuk, M., Qu, T., 2004. Seasonal variability of the large-scale currents near the coast of the Philippines\*. *J. Phys. Oceanogr.* 34 (4), 844–855. [https://doi.org/10.1175/1520-0485\(2004\)034<0844:SVOTLC>2.0.CO;2](https://doi.org/10.1175/1520-0485(2004)034<0844:SVOTLC>2.0.CO;2).
- Zhai, F., Hu, D., 2012. Interannual variability of transport and bifurcation of the north equatorial current in the tropical North Pacific Ocean. *Chin. J. Oceanol. Limnol.* 30 (1), 177–185. <https://doi.org/10.1007/s00343-012-1194-8>.
- Zuo, J., Zhang, M., Xu, Q., Mu, L., Li, J., Chen, M., 2012. Seasonal and Interannual Variabilities of Mean Velocity of Kuroshio Based on Satellite Data. <https://doi.org/10.3882/j.issn.1674-2370.2012.04.007>.